SHOALS3000 Surveying Above Dense Fields of Aquatic Vegetation – Quantifying and Identifying Bottom Tracking Issues

P. Kuus[1], J. Hughes Clarke[1], S. Brucker[1]
[1] *Ocean Mapping Group, University of New Brunswick*

Abstract

When a survey area is populated with biological growth such as kelp and seagrass, the range performance of lidar is challenged. Aquatic vegetation can lead to bottom miss-tracking or even absence of the optical signal return. The former results in shoal biased soundings; the latter results in datagaps. This last result is especially concerning, implying that marine life covered navigational hazards might appear as datagaps, while these are commonly assumed to be caused by lidar extinction depths. With ground truthing data (e.g. underwater photography, acoustics) vegetation presence or tracking of mid-water vegetation can be identified, although these datasets are commonly not available during a lidar survey. Incorporating characterized SHOALS3000 green laser waveform data yields a method to validate lidar soundings. This paper presents an assessment of the SHOALS3000 lidar bottom tracking performance in submerged vegetated areas, and a method to identify improper bottom tracking.

Introduction

This paper will address bottom tracking issues, and the recognition thereof, from the SHOALS3000 green laser operated above dense populated fields of Zostera marina and Laminaria sp.

Zostera marina is a seagrass that is commonly known as eelgrass, Laminaria sp. is species of the kelp family. Both types of vegetation grow in the Bay de Chaleur near the shores of Bonaventure and Paspébiac, Quebec, Canada. These shores have been mapped off- and onshore with a bathymetric lidar system, and offshore with a range of acoustic sounders (Kuus, 2008). The collected data were used for this study. Zostera marina or Laminaria sp., herein after refereed to as (aquatic) vegetation, can be detrimental to the success of a lidar sounding if it reflects from mid-water vegetation, or when the lidar signal fails to return. Both cases will degrade the quality of the terrain model due to an unreliable estimate of the seafloor, and a decrease in and inconsistency of the sounding coverage. An uncertainty is also introduced since the event of an incorrect sounding remains unknown without ground truthing data (e.g. acoustic bathymetry), which is, in fact, not commonly collected during lidar surveys. For survey areas such as the Bay de Chaleur we thus need to assess the bottom tracking ability of the lidar system in aquatic vegetated regions. In addition, we need to develop a method to identify improper bottom tracking due to aquatic vegetation from lidar data alone. The method proposed in this paper validates the lidar sounding by combining the bathymetry and green laser waveform data. First, the bottom tracking of the green laser is quantified. Next, the characterization process is discussed, followed by an explanation of the sounding validation process.

Survey

Airborne lidar and ship-based acoustic data were collected in Bay de Chaleur between June 21 and July 3, 2006 as part of the FUDOTERAM project. The Bay de Chaleur lies between the New Brunswick northern coast and the Gaspé, a peninsula of Quebec (Figure 1). Survey operations took place at locations near the towns of Bonaventure and Paspébiac in very shallow waters. Water depths ranged between 1.5 and 40 metres, although the majority of the survey area had an average depth of 6 metres, and towards the coast the survey launch (hereinafter referred to as the Heron) operated occasionally close to its navigable limits (~1.5m). The Heron was equipped with an EM3002 multibeam sonar (hereinafter referred to as multibeam), Knudsen 3.5 and 200 kHz singlebeam sonar and Knudsen 200 kHz keel mounted sidescan sonar. Ship-based data were acquired with moderate speeds of 4-7 knots during a 10 day deployment. As far as the water depths allowed, 100% seafloor ensonification was attempted. Mapping with such dense spacing was inefficient at extremely shallow depths (<8 m). In those cases, efforts were made to have at least full bottom sidescan coverage, i.e. lines adjoining swaths (line spacing ~80 m). An area was defined as the high density zone, referring to dense soundings of both acoustic and lidar bathymetry (Figure 1, box). In this area 100% multibeam ensonification was achieved, and it covers five smaller scale areas, which were populated by vegetation. These designated areas were mapped with 200% multibeam coverage and mainly intended for vegetation/bottom tracking analysis. The ship-based survey preceded the lidar over-flights by 1 to 12 days.

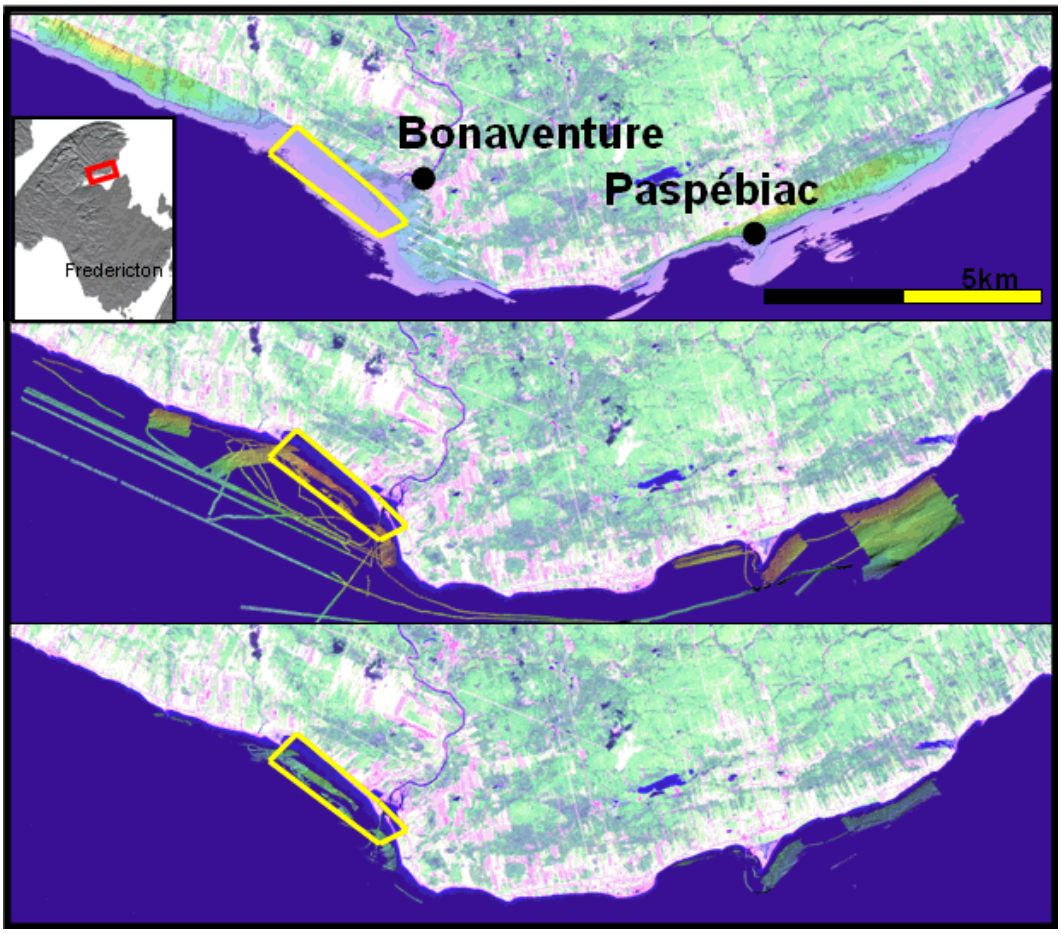

Figure 1 Landsat overview image of the survey area with lidar coverage (top), multibeam coverage (middle), and overlapping coverage (bottom). Bonaventure is located west where the Bonaventure river flows into the bay. The town of Paspébiac lies on the sharp elongation found easterly. The box in the upper image defines the high density zone.

The lidar coverage was largely focused on the shallow, near coastal, and land parts of the survey area. Lines with an approximate scan width of 150 m were flown above high density locations at Bonaventure and Paspébiac using ~125 m line spacing (2x2 m spot spacing) and thus overlapping 20% of the outer edges of adjacent scans. The remaining areas were mapped with a much larger scan width (275-300 m, 4x4 m spot spacing) and accordingly larger lines spacing (200 m), resulting in a near 50% overlap. The swaths above the high density locations consisted of 85 shots along the arc, which is less than the 100 shots usually applied at other locations.
Secchi disk measurements and Optech's Ocean Scientific prediction software estimated the green laser maximum depth penetration between 8 and 12 metres (Feygels, 2006). This proved to be a valid proxy.

Background

SHOALS bathymetric lidar

This study involves a SHOALS3000 bathymetric lidar manufactured by Optech, hereinafter referred to as lidar. It operates with two laser beams, an infrared and green beam, both produced coherently by the same infrared laser (using frequency doubling for the green beam). These two beams are reflected from a two-axis scanning mirror that distributes the laser beams as an arc shaped scan on the water surface. When the infrared laser beam (1064 nm) hits the water, it will not be able to propagate through the water column. The receiver will therefore only record returned intensity of the infrared laser beam backscatter on the water surface. The green laser beam (532 nm) can propagate through the water column as far as the optical water properties will allow. It, too, will produce a reflection on the water surface, but a portion of the emitted signal will also give a return from the bottom, or its first opaque medium (Figure 2). Differencing between (near vertical) travel times of the infrared laser beam surface detection and green laser beam bottom detection leads to the depth. A detailed description of the SHOALS lidar is given by Guenther (e.g. 1985, 2000, 2001).

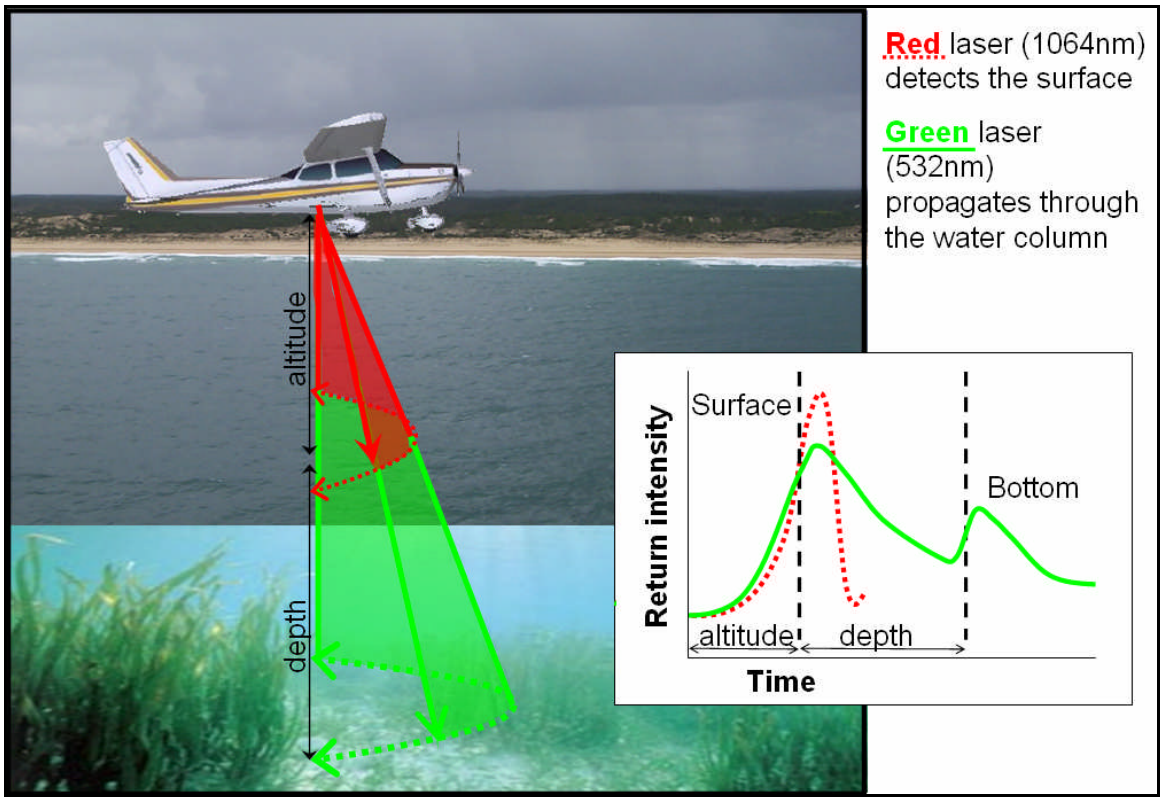

Figure 2 The principle of a bathymetric lidar system. It utilizes a near-infrared laser beam to determine the sea surface and a green laser beam to detect a reflector, ideally the seabed. A rotating mirror re-directs the laser, producing arc shaped swaths. The time series of a green laser beam typically shows a high peak identifying the sea surface return, and a second, usually smaller, peak as the bottom return. The returned signal decays as the range through the water column increases. Typical flight altitude 300 m, experienced depth range 2-13 m. Altitude and depth not to scale.

The SHOALS system records the waveforms of the received infrared and green laser returns in four channels: the infrared channel, two channels for the green laser at different fields of view (FOV) namely, the PMT (Photomultiplier Tubes) and GAPD (Gated Avalanche Photodiode) channel, and the green excited Raman channel used for a more accurate surface detection. The returned signal amplitudes are originally measured in linear units but logarithmically compressed into unsigned 8bit digital numbers to cope with the enormous dynamic range in the signal. The signal is digitized at 1ns intervals, this translates to a range sampling interval of 0.115 m.

Previous work

Lidar sounding accuracy studies and comparisons with acoustic (swath) bathymetry have been documented before (e.g. Hare, 1994; Riley, 1995; Guenther et al., 1996a; LaRocque et al., 2004; Optech Inc., 2004; Lockhart et al., 2005). An assessment of the SHOALS3000, however, has not been published yet, although the achievable depth accuracy should lie within 50.0 cm 2σ (Optech Inc., 2006). Research on lidar accuracy has paid specific attention to the detection of small navigation hazards (~2 – 1 m), and improvements to limit object detection failure (Guenther, 2001; Guenther et al., 1996b; Steinvall, 1996). The detection of aquatic vegetation, inherently a failure of the bottom tracking, and a practical assessment thereof has not been commented upon.

With the availability of laser waveforms associated with each sounding, the seabed can be segmented based on the waveform characteristics. Waveform characterization has been done

by several researchers (Wang and Philpot, 2002; Lee and Tuell, 2003; Dijkstra and Elston, 2004; Wang, 2005) although each used a different technique. The characterization method described in this paper, for example, required an algorithm that adapted as well as possible to lidar returns from vegetated seabeds, and yielded an estimate for the water clarity as by-product.

Results and Discussion

Bottom tracking

The lidar bottom tracking assessment involved multibeam bathymetry and water column backscatter, and Knudsen 200 kHz singlebeam water column backscatter. Although previous experience showed the multibeam can have difficulties in penetrating particular densely layers of aquatic vegetation, this work showed that under typical densities the multibeam can correctly track the seabed. As the vegetation did not hinder the multibeam's bottom tracking (confirmed from examining the water column image), it acted as a reference against lidar data for its bottom tracking assessment. Post processed kinematic (PPK) antenna solutions were allocated to ensure accurate vertical positioning, thus also accounting for tides. The multibeam bottom tracking assessment and PPK processing fall out the scope of this paper, but readers are referred to Kuus (2008).

In demonstrating the bottom tracking performance of the lidar, one example that represents the complete dataset, is evaluated here. The chosen study area contains dispersed vegetation populations, but mainly on, or close to, the vicinity of a rock ridge. The study area was surveyed with 200% multibeam coverage and Knudsen 200 kHz singlebeam, and showed sufficient overlap with lidar soundings (Figure 3). Longitudinal profiles of lidar and multibeam were compared with Knudsen backscatter (Figure 4). The multibeam profiles follow the strongest Knudsen backscatter, which indicates the underlying seabed. The rock ridge is clearly recognized in both multibeam profiles. Lidar profiles illustrate two events of bottom tracking failure at the presence of vegetation: 1) tracking of the vegetation, and 2) absence of a return:

1) *Tracking of vegetation* – The lidar profiles appear noisier than multibeam, and shallow peaks match with high Knudsen backscatter, especially above the rock ridge where dense vegetation populations are present. In the top example (A-B), the lidar profile above the rock ridge matches vegetation backscatter precisely. The vegetation blocks the green laser light, and the remainder of the signal is absorbed and scattered, decreasing the chance of a successful penetration towards the seabed. The dark color of the vegetation promotes the blocking of the green laser light as well.
2) *Absence of a return* – The lower portion of the area in Figure 3 shows many datagaps. Multibeam bathymetry did not indicate extreme depths (i.e. depths exceeding the extinction depth, ~13 m) at these datagaps. Moreover, the lidar was able to produce soundings at similar depths elsewhere. Waveforms around datagaps did not illustrate a volume return slope change, which would indicate a water clarity problem. While water column scattering clearly reveals mid-water vegetation (Figure 4, profile C-D), it is apparent that the presence of vegetation (possibly in combination with an increase of depth) results in the absence of a laser return.

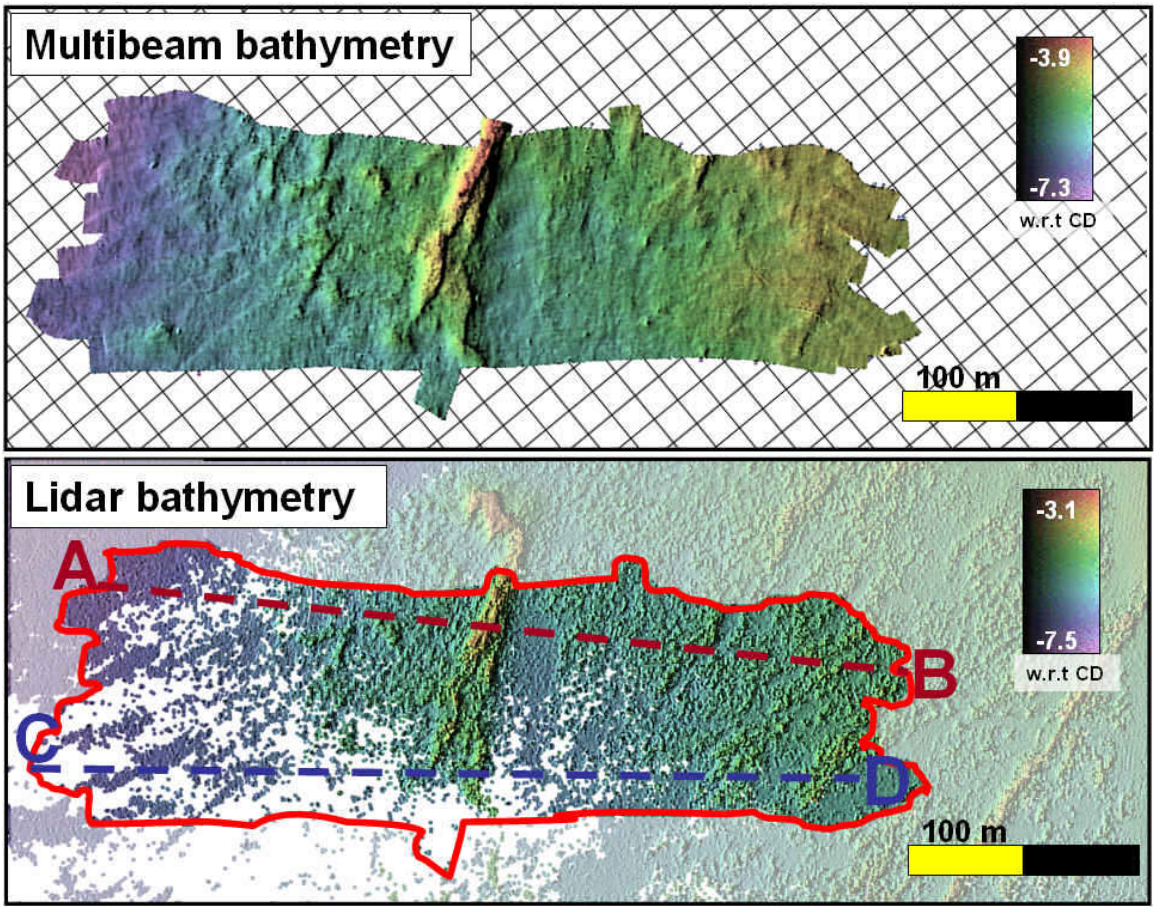

Figure 3 Multibeam (top) and lidar (bottom) bathymetry. Overlapping multibeam coverage on the bottom image is displayed unshaded. A rock ridge divides the area in the middle. The vegetation is known to populate the rocks. Lines A-B and C-D correspond with longitudinal profiles in Figure 4. Background grid size is 25 m.

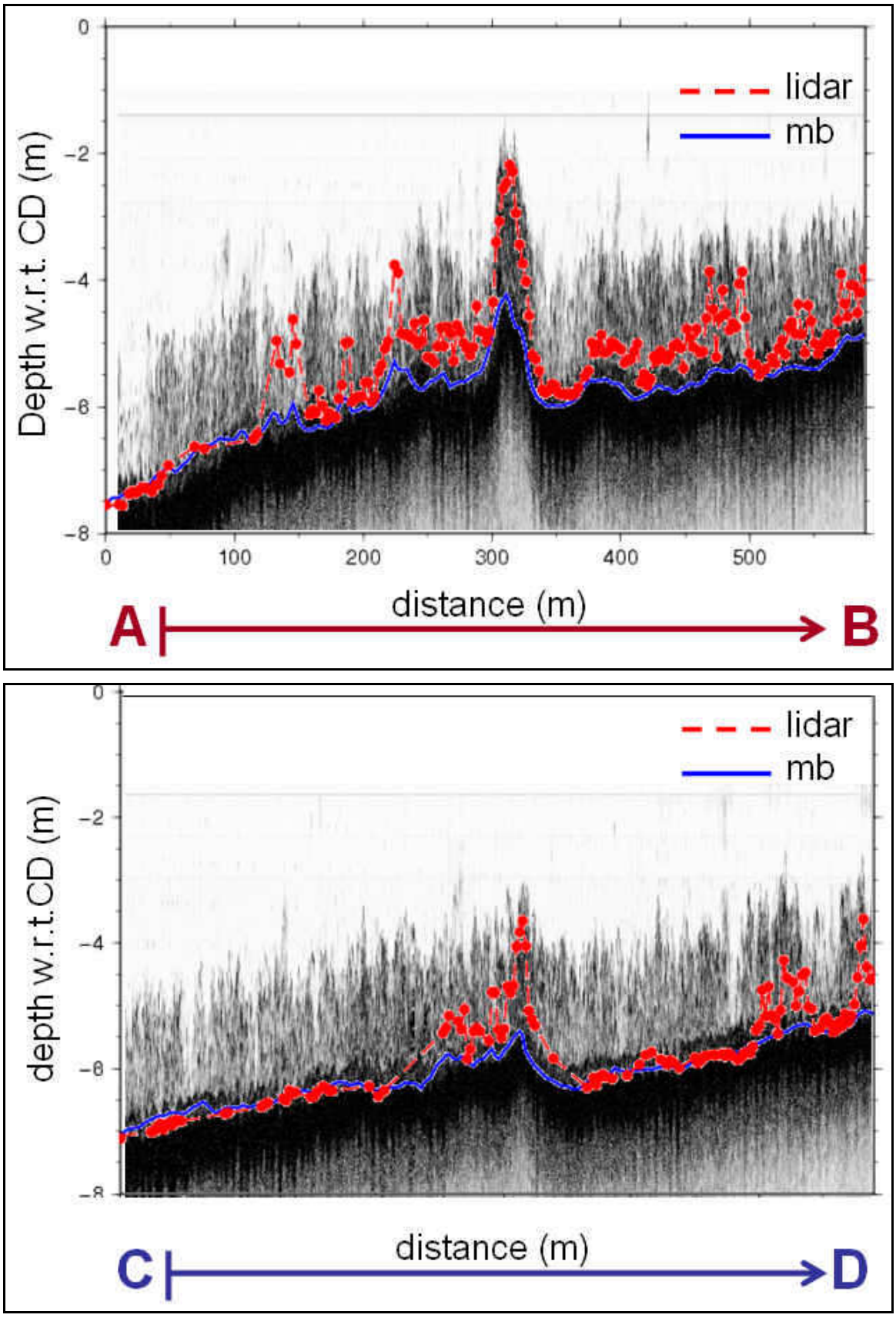

Figure 4 Two sets of longitudinal profiles corresponding with the dashed lines in Figure 5.7. Lidar (dashed red) and multibeam (blue) bathymetry is plotted with Knudsen 200 kHz singlebeam backscatter as background. Successful lidar returns are plotted with a red dot. Note the slight mismatch of multibeam and Knudsen seafloor in the C-D profile. This is likely due to a bend in the ship track. Knudsen data

follows exactly the ship's track, whereas the multibeam profile contains depths extracted from a straight line between C and D.

Quantitative analysis

For the quantitative analysis two area types were defined: 1) bottom tracking in areas where no vegetation was identified with ground truthing data, typed as "vegetation free" areas; and 2) bottom tracking at vegetation presence: "vegetation rich" areas. The results from the subtraction of lidar from multibeam digital terrain models (DTM) are presented in Table 1. The mean depth differences and standard deviations found at vegetation free locations are similar to those seen in other assessment studies that included a multibeam as reference (e.g. LaRoque et al., 2004, Lockhart et al., 2005). The result of the lidar tracking on the vegetation canopy, as seen in the examples above, is found back in the statistics in Table 1; at vegetation rich areas a large *positive* mean and standard deviation results. Also, presented in Table 1 are the depths ranges of both systems. The depth range of the lidar soundings compared to the depth range of multibeam soundings in vegetation rich areas indicate two things: 1) shallower lidar soundings due to tracking on the vegetation canopy, which, in fact, confirms with the example profiles above and the statistics in Table 1, and 2) limited maximal achievable depth. This second observation is ultimately the result of the absence of a lidar return and usually only occurs when the green laser reaches its optical depth. The far right column in Table 1 presents the percentage of empty grid cells in the lidar DTM compared to the multibeam DTM. In areas without vegetation (and without depths exceeding the optical depth) the failures of lidar returns are insignificant and the data absence compared to multibeam data is near zero. In the vegetated areas included for the DTM analysis, however, the lidar data absence increased to 11 %.

Table 1 Results from differencing between lidar and multibeam DTM's, positive mean depth difference indicating lidar measuring shallower than the multibeam.

	$\Delta\bar{d}$ (m)	$\sigma_{\Delta d}$ (m)	Coverage (m^2)	Lidar depth range (m)	MB depth range (m)	Data absence (%)
Vegetation free	+0.05	0.15	1493468	2 – 11	2 – 11	0
Vegetation rich	+0.44	0.42	218475	1 – 8	2 – 9	11

Once again we use the same area as above to show the effect of vegetation presence on the lidar DTM (Figure 5). Note that this area is not categorized as purely vegetation rich; the area exhibits varying densities of vegetation populations. Due to this variation, the mean depth difference is less than for a purely vegetation rich area, though still significant, +0.38 m with standard deviation 0.45 m. The bathymetry in the examined area would, due to vegetation presence, greatly exceed IHO Order 1 accuracy norms (±0.99 m (95%) at 7.5 m depth) and the specifications of the SHOALS3000 system (<0.50 m 2σ): $\Delta\bar{d} + 2\sigma_{\Delta d} = 1.28m$. Moreover, the examined lidar DTM includes many datagaps (20.2 %), mainly in the deeper portion of the area.

A visual inspection of the lidar, multibeam, and histogram DTM in Figure 5 show spiky, or disturbed regions in the lidar data corresponding with larger positive (thus shallower) depth differences. The largest discrepancies are seen on the rock ridge, where singlebeam acoustics and multibeam water column imaging identified the majority of the vegetation. In fact, high positive bins (~>1.6 m) on the rock ridge are approximately equal to the height of the vegetation measured from the Knudsen 200 kHz profiles. As a comparison, Figure 5 also

includes the histogram of a vegetation free area ($\Delta\bar{d}$ = +0.11 m, $\sigma_{\Delta d}$ = 0.18 m, area = 269148 m^2).

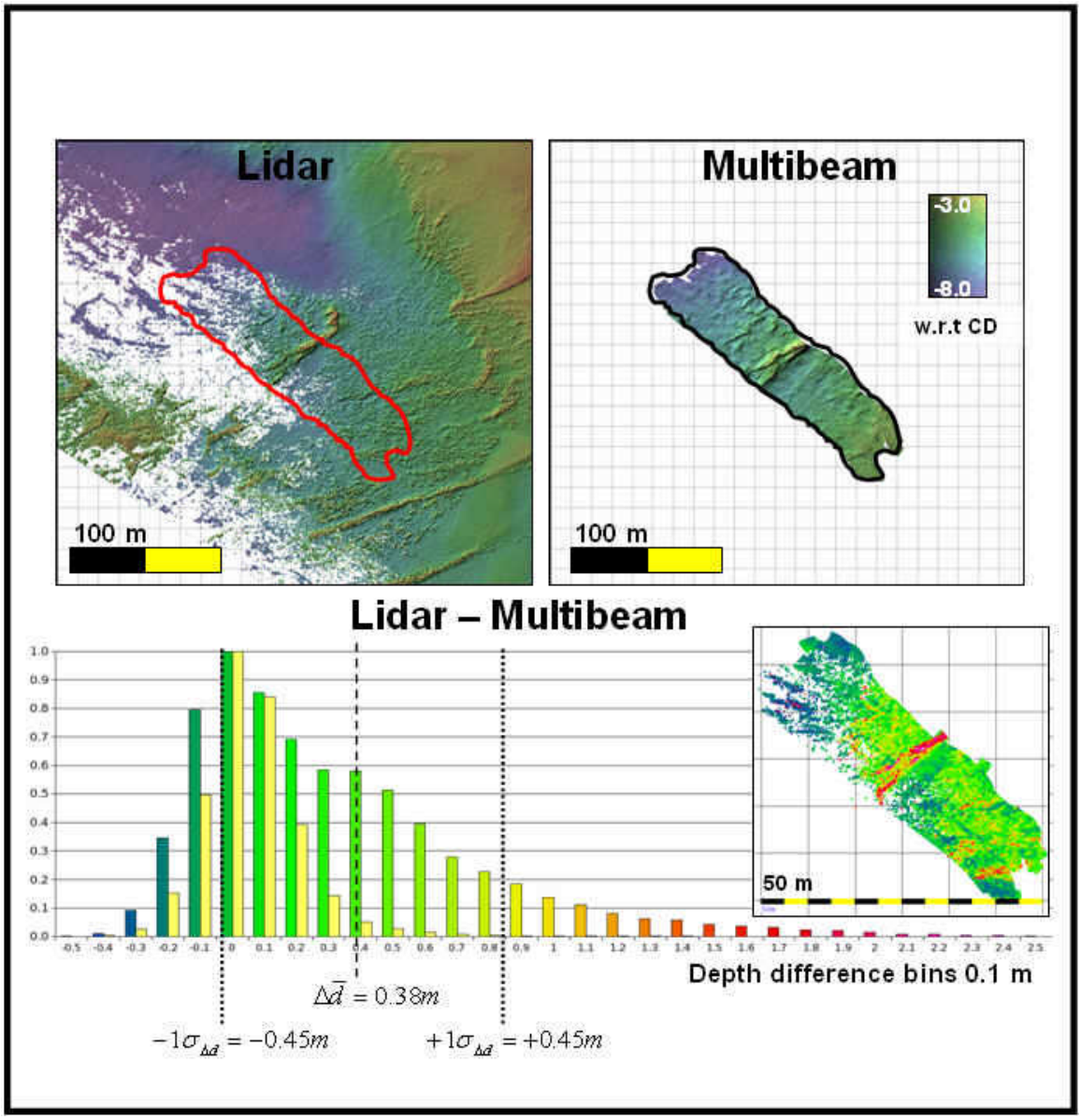

Figure 5 Lidar (top left) and multibeam (top right) DTM of a mixed vegetation free and vegetation rich area. The red line in the lidar DTM bounds the multibeam overlap. The normalized histogram shows depth differences of a vegetation free area (yellow bars, $\Delta\bar{d}$ = +0.11 m, $\sigma_{\Delta d}$ = 0.18 m, area = 269148 m^2) and of the subtraction of the upper lidar and multibeam DTM's ($\Delta\bar{d}$ = +0.38 m, $\sigma_{\Delta d}$ = 0.45 m, area = 107296 m^2, data absence = 20.2 %). The lower right DTM presents the color coded histogram bins.

Characterization

An algorithm was developed that characterizes the green laser waveform based on the bottom return height. A typical lidar waveform consists of the surface return, the water column or volume return, and finally the bottom return (Figure 6). The bottom return height, essentially the optical backscatter, is determined as the height of the bottom return relative to the attenuation curve, the extrapolation of the volume return. The slope of the attenuation curve is

in fact a proxy for the water clarity. This by-product of the characterization process allowed us to generate water clarity maps, although these are not discussed in this paper. Environmental effects on waveform data have been investigated (seabed slope, surface topography, water clarity, and depth), but none of these factors required accounting for. By measuring the bottom return height relative to the extrapolated attenuation curve in logarithmic units, water clarity and depth effects were almost removed. The algorithm required a series of techniques in order to distinguish a bottom return from vegetation waveforms. If a bottom return could not be detected (e.g. too shallow depths), the waveform was flagged as invalid and omitted from the characterization process. The logarithmic bottom return height excess over the attenuation are extracted from all valid flagged waveforms and spatially plotted; thus, log height is used as a relative measure of the inherent optical backscatter strength of the seabed. Ground truthing data proved that regions with small optical backscatter matched with vegetation presence. Although natural variability in optical backscatter was seen over different physical seabeds (mud, sand, gravel), the optical backscatter of vegetation falls clearly below any of these unvegetated seabed types. The optical backscatter of overlapping areas did show day-to-day changes (possibly due to imperfect reduction for source pulse (assumed constant) altitude or waterclarity), but the ratio of optical backscatter from vegetated and unvegetated areas remained the same, by which ratio low optical backscatter could confidently be linked to aquatic vegetation.

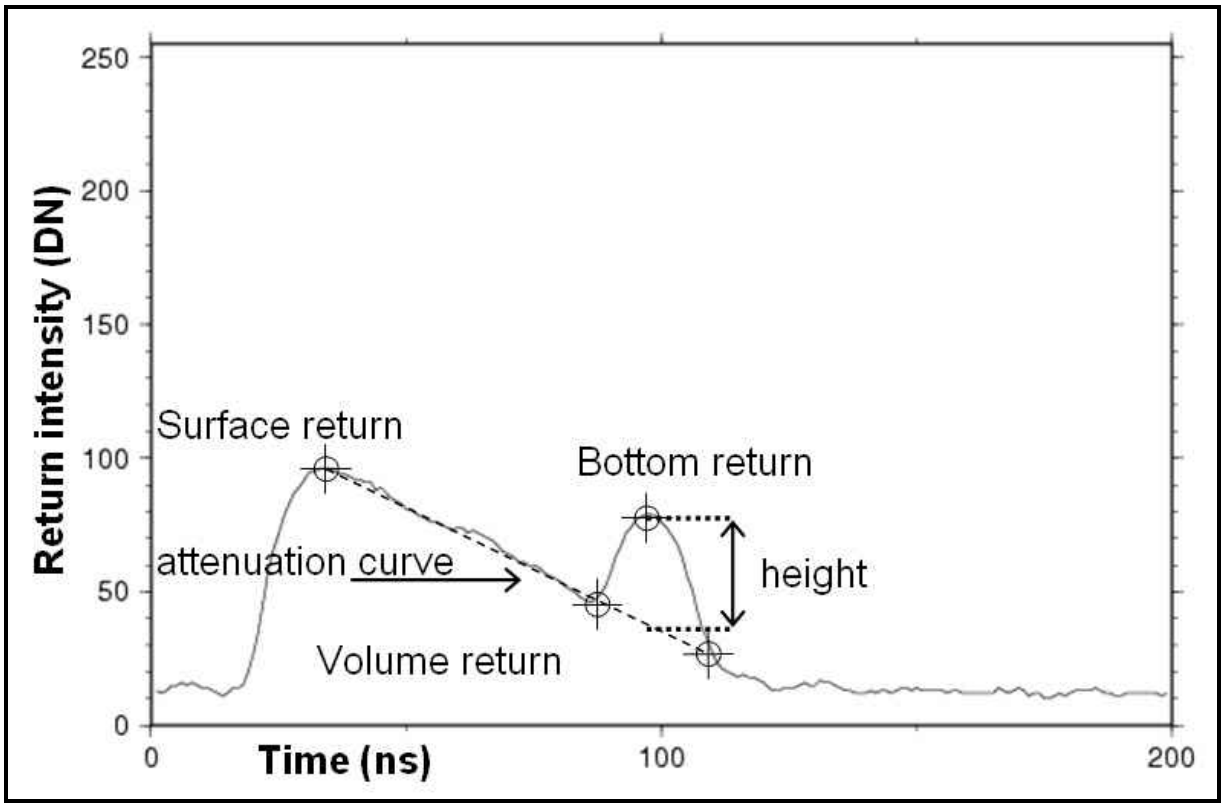

Figure 6 Typical lidar waveform, consisting of a surface, volume, and bottom return. The optical backscatter is defined as the height of the bottom return relative to the attenuation curve.

An example of the derived optical backscatter map is presented in Figure 7 (middle). The optical backscatter map illustrates regions with low backscatter corresponding to fields of vegetation seen in aerial photography (Figure 7 top). Also depicted in Figure 7 are underwater photography portraying a vegetated seabed when optical backscatter is low or waveform data is missing, and an unvegetated seabed when optical backscatter is much higher. Waveforms

close to the shallow coast were flagged as invalid due to a merged surface and bottom return and therefore do not appear on the map. Datagaps seen within the flight lines, however, truly represent missing data. At these locations, lidar soundings and their associated waveforms were not provided since a depth could not be determined. While usually at such datagaps, depths are assumed to exceed the lidar extinction depth, in these cases the vegetation appears to limit the lidar's penetration. This event was demonstrated with overlapping keel mounted sidescan sonar backscatter data. Lidar datagaps occurred above patches of high acoustical backscatter (Figure 8), which represented rock formations or pebble covered seabeds, inherently potential habitats of rock based vegetation such as Laminaria sp. (Figure 8d1). Although acoustical sidescan backscatter cannot easily be used to identify the vegetation itself, acoustical backscatter can identify the substrate on which the vegetation grows.

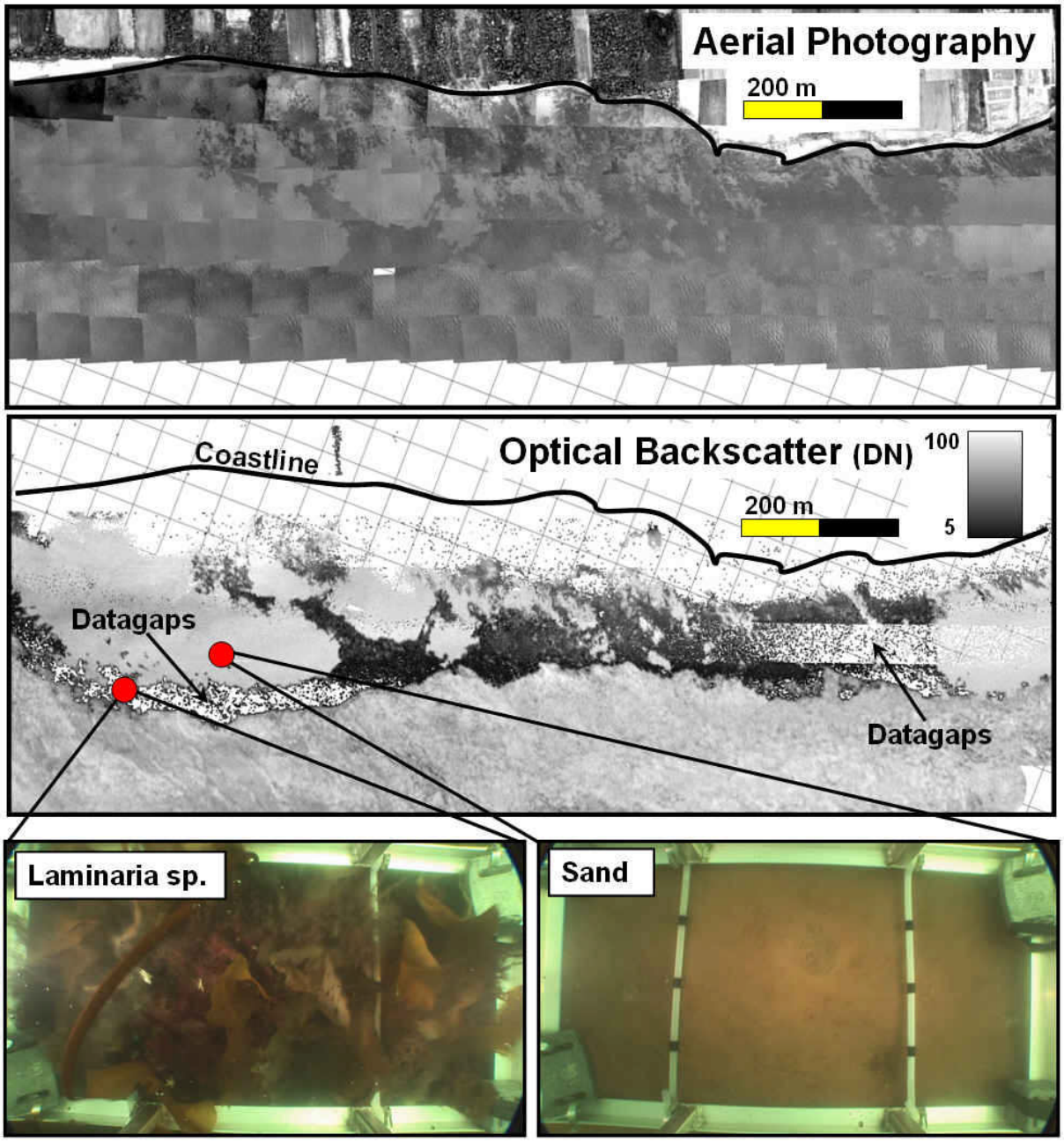

Figure 7 Fields of aquatic vegetation recognized in aerial photography (top) match with regions of low optical backscatter (middle). Invalid flagged waveforms (e.g. waveforms with a merged surface and

bottom return) in the shallow zone are disregarded by the algorithm. Underwater photography (bottom) confirms the presence of vegetation at low optical backscatter or datagaps.

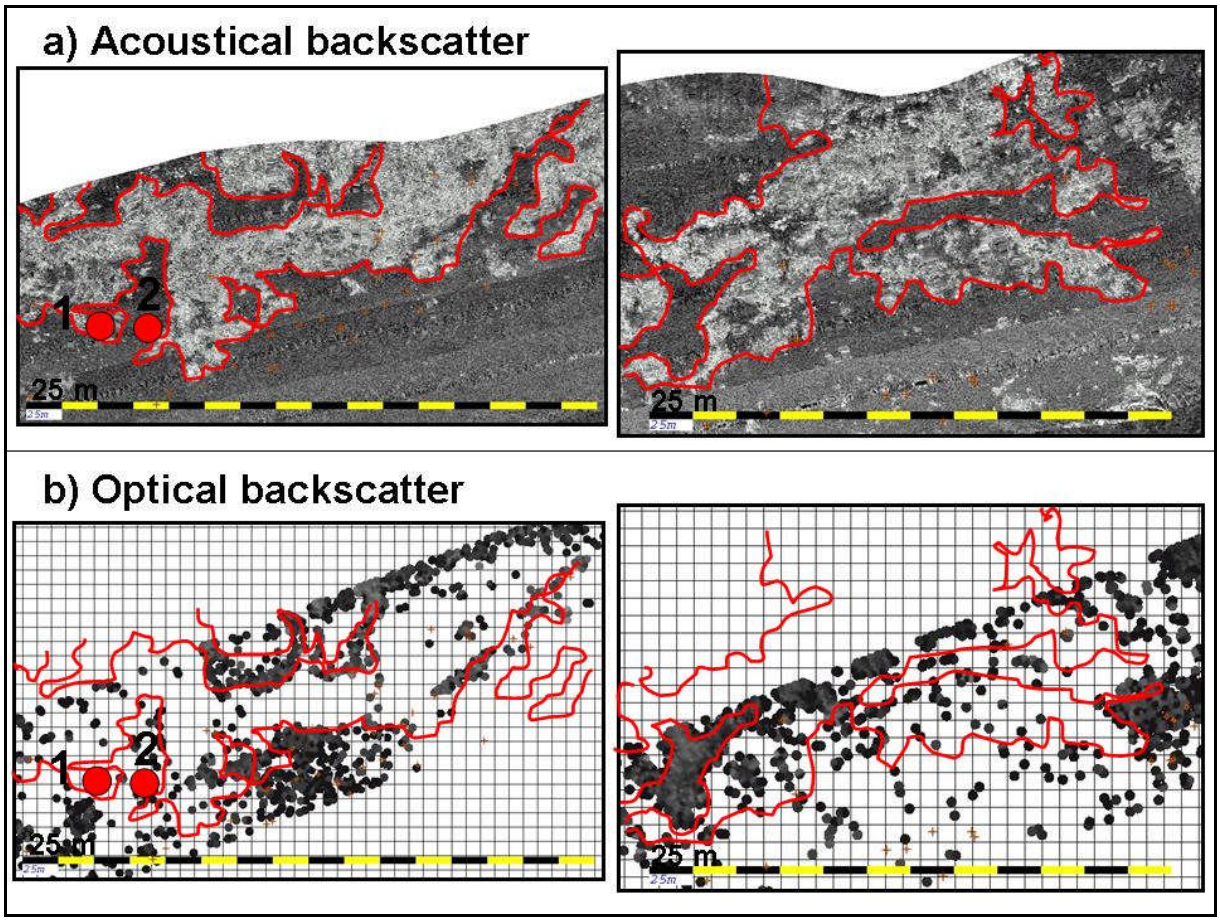

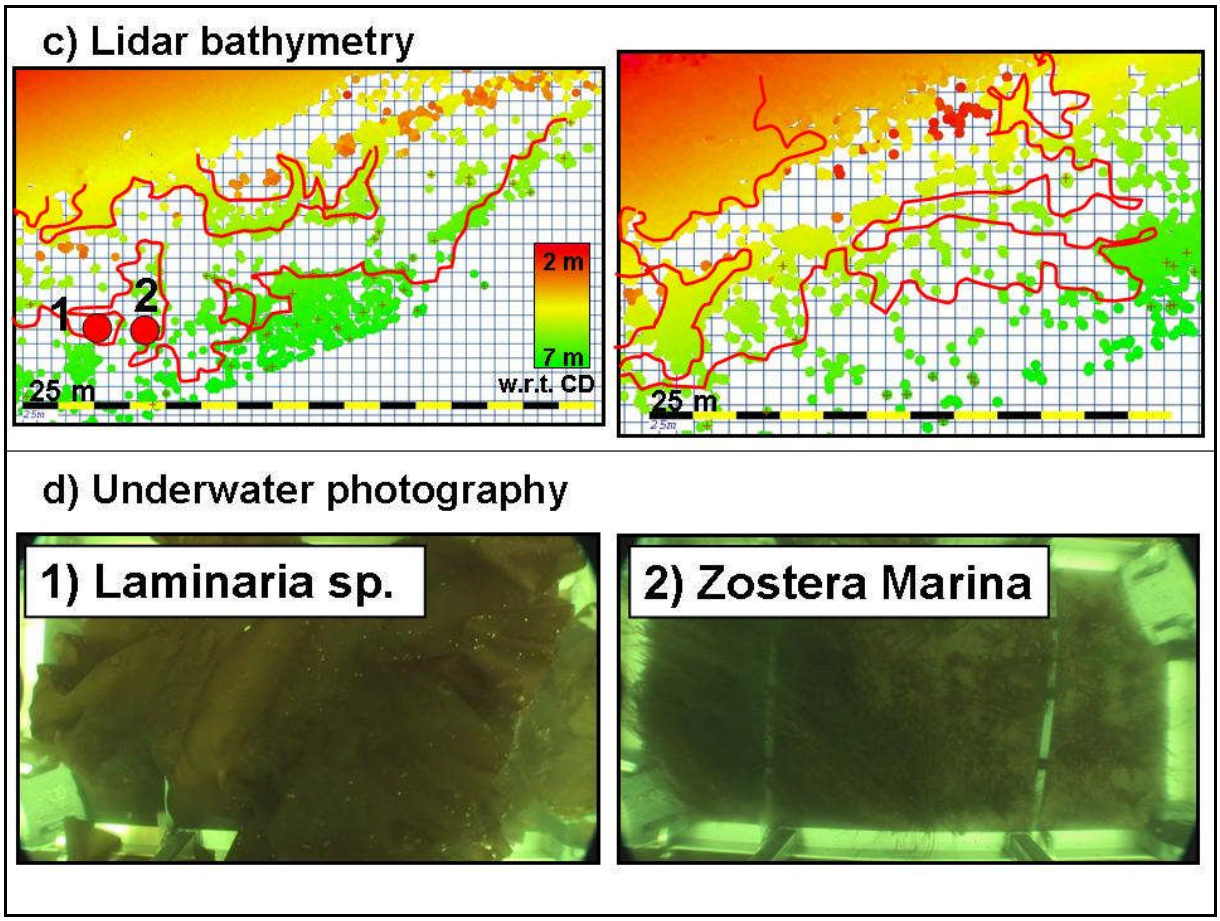

Figure 8 Overlapping a) acoustical backscatter, b) optical backscatter, and c) lidar bathymetry. The contour of high acoustical backscatters (representing rock formations) circumvents the lidar datagaps. Underwater photography reveals rock based vegetation at lidar datagaps and high acoustical backscatter (d1), and sand based vegetation at lidar datagaps with a low acoustical backscatter (d2).

Validation

As demonstrated above, two important phenomena occur when the green laser beam strikes on vegetation: 1) low optical backscatter (OBS), and 2) bottom mis-tracking. In addition, acoustic backscatter can reveal potential habitats of vegetation. These phenomena were used in an automated logic to assess lidar datasets. The logic includes threshold (T) values of the lidar bathymetry slopes (between adjoining grid cells), optical backscatter, or acoustical backscatter (ABS), and is based upon raster images of the slopes or acoustical backscatter against a raster image of the optical backscatter. The logic compares overlapping grid cells (xy) against threshold values and then determines a classification. When lidar bathymetry slopes (indicator of rapid variations in depth) and optical backscatter is used, the following logic is invoked:

Table 2 Logic for validation based on lidar bathymetry slope and optical backscatter.

Logic	Classification
$xy_{slope} > T_{slope}$ and $xy_{OBS} < T_{OBS}$	Tall growing vegetation, or marine life covered navigational hazard
$xy_{slope} < T_{slope}$ and $xy_{OBS} < T_{OBS}$	Low growing vegetation, or tracking vegetation canopy

$xy_{slope} > T_{slope}$ and $xy_{OBS} > T_{OBS}$	Valid sounding, but potential navigational hazard
$xy_{slope} < T_{slope}$ and $xy_{OBS} > T_{OBS}$	Valid sounding

When the green laser starts to track the vegetation, the slope of the DTM between adjoining grid cells will increase. If the green laser tracks on top of the vegetation, the slope will change irregularly but may lie below the slope threshold. However, the returned waveform will have a decreased optical backscatter suggesting a vegetated seabed. Natural seabed topography passes the validation, while seabed objects (e.g. wreck, anchor) covered by marine life, would be classified as distrustful soundings. Vegetation classified soundings should therefore always require the hydrographer's awareness. Unfortunately, the data used for this study did not include any (manmade) seabed objects to test the logic for this specific case.
A similar logic was formulated for overlapping acoustical backscatter and optical backscatter data (Table 3). Overlapping acoustical backscatter indicates vegetation habitats, from which it is possible to localize vegetation species.

Table 3 Logic to determine vegetation habitats.

Logic	Classification
$xy_{ABS} > T_{ABS}$ and $xy_{OBS} < T_{OBS}$	Pebble- or rock-based vegetation
$xy_{ABS} < T_{ABS}$ and $xy_{OBS} < T_{OBS}$	Sand-based vegetation
$xy_{ABS} > T_{ABS}$ and $xy_{OBS} > T_{OBS}$	Unvegetated pebbles or rocks
$xy_{ABS} < T_{ABS}$ and $xy_{OBS} > T_{OBS}$	Unvegetated sand

One example of the validation scheme is presented here (Figures 9 to 13). The bathymetry shows spiky or irregular topography, mainly around the linear features in the southern part. These features were identified as rock ridges by acoustical bathymetry and water column scattering. The rock ridges also stand out in the optical backscatter map. When the bathymetry and optical backscatter are combined, we can segment the dataset in an unvegetated seabed, or tall or low growing vegetation. It appears, for example, that the rock ridges are populated with tall growing vegetation. A more important observation is the large clusters of vegetation classified soundings. With such large clusters of untrustworthy soundings, this lidar dataset appears less efficient in terms of data coverage and safety of navigation purposes. However, should some kind of approximation of vegetation presence be a desirable product, then this lidar dataset would be a benefit to ecological mapping. Building on this last comment, although overlapping acoustical backscatter is not usually incorporated with lidar surveys, acoustical backscatter adds an extra degree of freedom to the classification as it allows us to segment vegetation species based on their potential habitats.

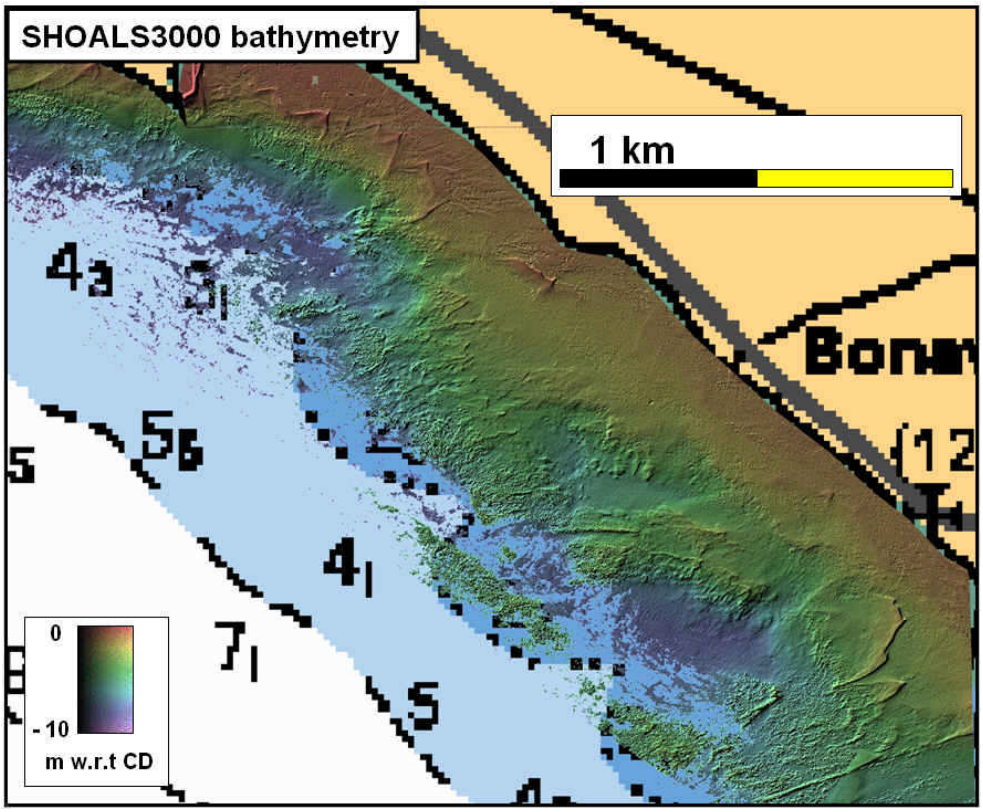

Figure 9 SHOALS bathymetry along the Bonaventure coast. Background chart depths are in fathoms.

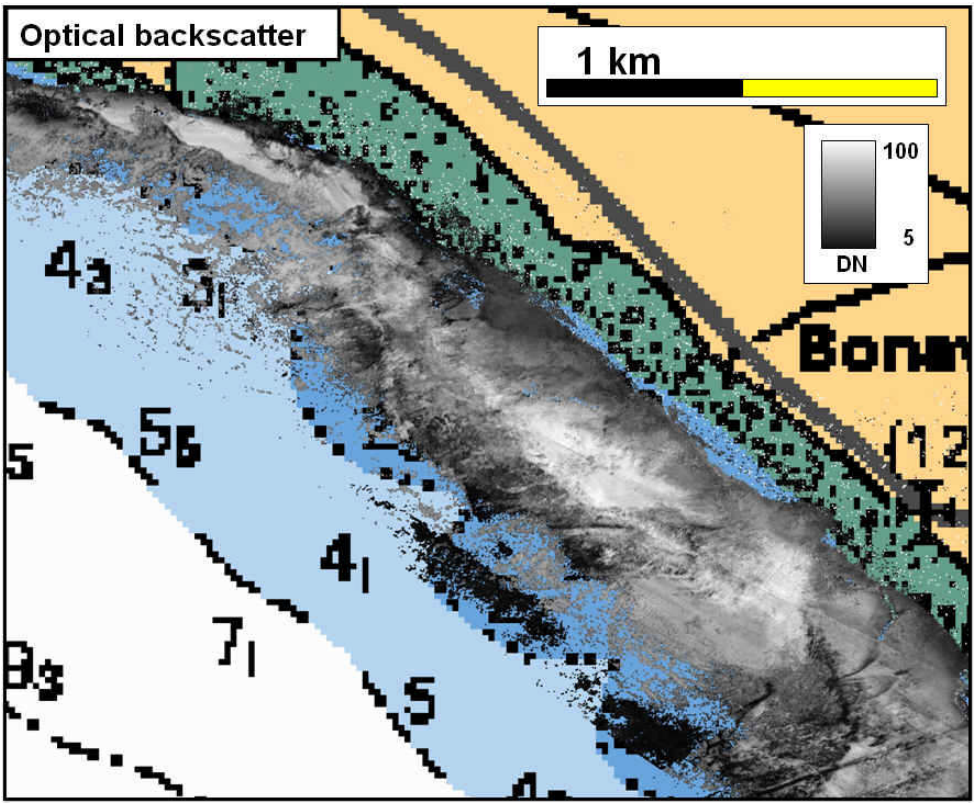

Figure 10 Optical backscatter. Waveforms that were not considered suitable for the characterization (e.g. too shallow depths) are omitted.

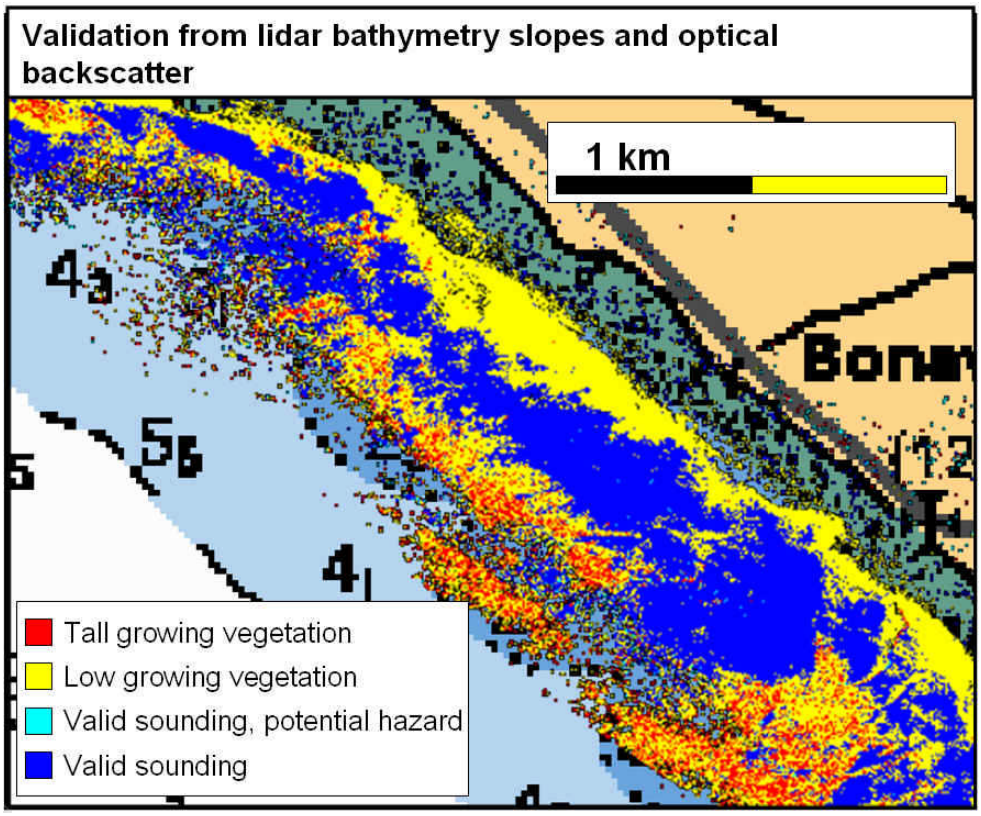

Figure 11 Sounding validation based on the bathymetry slopes and optical backscatter.

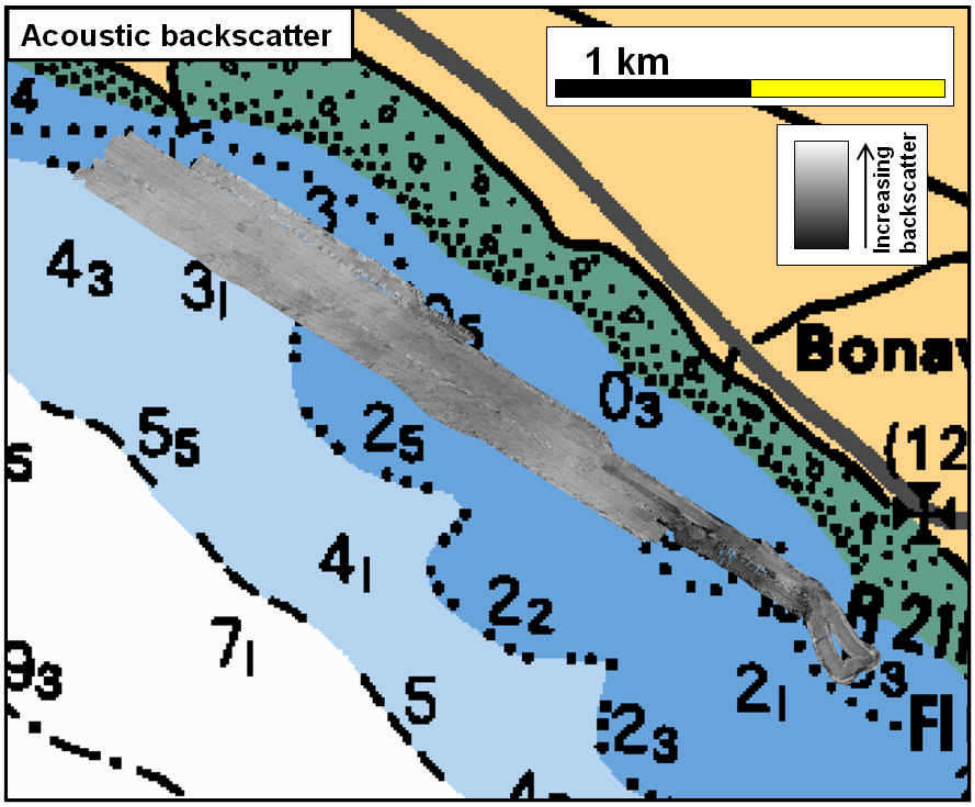

Figure 12 Overlapping keel mounted side scan sonar backscatter

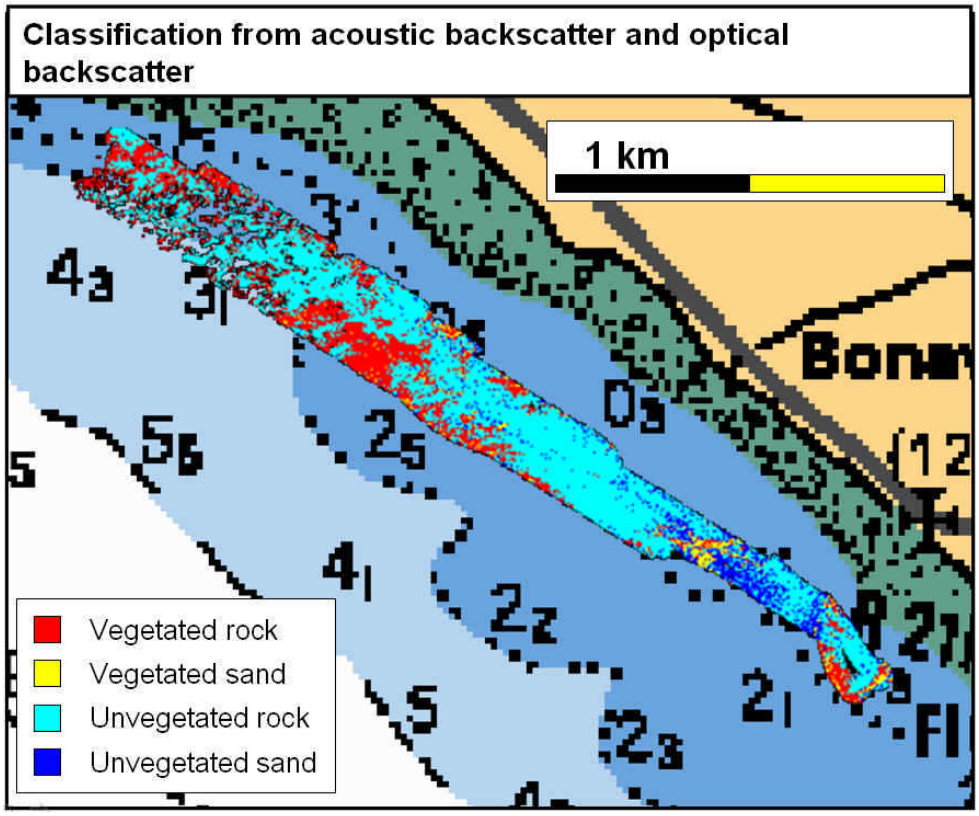

Figure 13 Classifying the data from acoustical and optical backscatter.

Conclusion

The presence of vegetation limits the penetration of the green laser signal in two ways: 1) masking the signal from the seabed, thus causing the lidar to measure the vegetation canopy instead, resulting in shoal biased soundings, and 2) reducing the return signal strength in such a way that the lidar system potentially cannot detect a bottom return, therefore causing gaps in the data. This last effect is the most concerning, not only because the effective coverage, typically a great asset of bathymetric lidar, is reduced, but also because lidar datagaps do not necessarily result from depth and/or water clarity issues, but could represent marine life covered navigation hazards. Moreover, data from lidar systems that associate unsuccessful lidar soundings with a "no bottom at" statement, may do the hydrographers' judgment more harm than good.

A proposed method to validate lidar soundings in densely vegetated areas when ground truthing data were unavailable includes characterized waveforms. Image based thresholding, including bottom return height and lidar bathymetry slopes, was used to classified regions in terms of vegetation presence and seabed topography. In addition, acoustical backscatter provides extra information about the substrate that the vegetation populates. This method has a potential to discriminate tall or low, and sand- or pebble-/ rock-based vegetation.

Acknowledgments

The first author would like to thank Capt. Serge LeMay, Steve Brucker and, Marketa Porkona for their invaluable assistance during the data collection on the Heron. This research was supported by funding from the Canadian Network of Centres of Excellence GEOIDE and

sponsors of the Chair in Ocean Mapping at UNB: US Geological Survey, Kongsberg Maritime, Rijkswaterstaat, Fugro Pelagos, Royal Navy and the UK Hydrographic Office, Route Survey Office of the Canadian Navy, Centre for Coastal and Ocean Mapping, and the Canadian Hydrographic Service. The SHOALS3000 was provided by the US Navy and operated by Dynamic Aviation for the US Navy. SHOALS3000 data were processed by Optech Inc.

References

Dijkstra, S.J., Elston, G.R., (2004). "Bottom Segmentation and Classification Using Expectation-Maximization Clustering Methods on SHOALS Data". *Conference Proceedings: American Society for Photogrammetry and Remote Sensing*, Denver, CO, 23 - 28 May, 2004, 11 pp.

Feygels, V.I., (2006). "Prediction of SHOALS-1000 Performance in Bay de Chaleur (Quebec) Region." Optech International Inc.

Guenther, G.C., (1985), Airborne Laser Hydrography, System Design and Performance *Factors*. NOAA, Rockville, U.S.

Guenther, G.C., Thomas, R.W.L., LaRocque, P.E., (1996a). "Design Considerations for Achieving High Accuracy with the SHOALS Bathymetric Lidar System." *SPIE Laser Remote Sensing of Natural Waters from Theory to Practice*, volume 2964, pp 26–37.

Guenther, G.C., Eisler, T.J., Riley, J.L, Perze, S.W., (1996b). "Obstruction Detection and Data Decimation for Airborne Laser Hydrography." *Proceedings of the Canadian Hydrographic Conference*, Halifax, N.S., 15 pp.

Guenther, G.A., Cunningham, A.G., LaRocque, P.E., Reid, D.J., (2000). "Meeting the Accuracy Challenge in Airborne Lidar Bathymetry." *Proceedings of EARSeL – SIG – Workshop LIDAR, Dresden/FRG*, June 16 – 17, 27 pp.

Guenther, G.C., (2001), "The DEM Users Manual", Chapter 8 Airborne Lidar Bathymetry, pp 236-307.

Hare, R., (1994). "Calibrating LARSEN-500 Bathymetry in Dolphin and Union Strait using dense Acoustic Ground-Truth." *International Hydrographic Review*, Monaco, volume LXXI(1), March 1994. pp 91-108.

Kuus, P., (2008). *Bottom Tracking Issues and Recognition Thereof using SHOALS3000 Green Laser in Dense Fields of Zostera Marina and Laminaria sp.* M.Sc.E.thesis, Department of Geodesy and Geomatics Engineering, University of New Brunswick, Fredericton, N.B., Canada, 230 pp.

LaRocque, R.E., Banic, J.R., Cunningham, A.G., (2004). "Design description and field testing of the SHOALS-1000T airborne bathymeter." *Proceedings SPIE* volume 5412, *Laser Radar Technology and Applications IX*, pp162-184.

Lee, M., Tuell, G., (2003). "A Technique for Generating Bottom Reflectance Images from SHOALS Data." *Proceedings U.S. Hydrographic Conference*, Biloxi, Mississippi, 2003, 13 pp.

Lockhart, C., Arumugam, D., Millar, D., (2005). "Meeting Hydrographic Charting Specifications with the SHOALS-1000T Airborne Lidar Bathymetry." *U.S. Hydrographic Conference Proceedings*, San Diego, California, 2005, 8 pp.

Optech Incorporated, (2004). Field Test Report for CHARTS, contract number: DACW42-01-C-0023, 82 pp.

Optech Incorporated, (2006). *SHOALS3000 Specifications*, 2pp.

Wang, C.K., Philpot, W.D., (2002), "Using SHOALS LIDAR System to Detect Bottom Material Change". *Geoscience and Remote Sensing Symposium, IGARSS'02, IEEE*, volume 5, pp.2690-2692.

Wang, C.K., (2005). “Ocean Bottom Characterization Using Airborne LIDAR: Monte Carlo Simulation and Investigation of Bottom Material Reflectance/Fluorescence.” Ph.D dissertation, Cornell University, Ithaca, New York, 97 pp.

Author Biographies

Pim Kuus is a graduate student with the Ocean Mapping Group. He is currently finalizing his master’s research which involves bathymetric lidar and multibeam. He holds a BSc degree in hydrographic surveying from the ‘Maritiem Instituut Willem Barentz’ on Terschelling, the Netherlands.

P.O. Box 4400
Fredericton, New Brunswick
Canada E3B 1N9
Fax: 506-453-4943
Phone: 506-453-3576
pimk@omg.unb.ca

John Hughes Clarke is the Chair in Ocean Mapping and a professor in the department of Geodesy and Geomatics Engineering at the University of New Brunswick. He holds degrees in geology and oceanography from Oxford, Southampton, and Dalhousie.

Steven grew up on northern Vancouver Island and in the Kootenay region of British Columbia. He moved to Fredericton, New Brunswick in 2001 to attend the University of New Brunswick where he completed a BScE in 2005. His hydrographic experience includes several arctic voyages aboard the CCGS Amundsen, west coast surveys of the Squamish River delta, and much local N.B. work aboard the CSL Heron. He's currently a research assistant with the Ocean Mapping Group at UNB and is working part time on a MScE.